IEEE Open Journal of
Intelligent Transportation
Systems

Received 29 August 2023; revised 13 October 2023; accepted 21 November 2023. Date of publication 24 November 2023;
date of current version 12 December 2023.

Digital Object Identifier 10.1109/OJITS.2023.3336464

Toward Safer Autonomous Vehicles: Occlusion-Aware Trajectory Planning to Minimize Risky Behavior

RAINER TRAUTH [1,3], KORBINIAN MOLLER [2,3], AND JOHANNES BETZ [2,3] (Member, IEEE)

[1]Institute of Automotive Technology, Technical University of Munich, 85748 Garching, Germany

[2]Professorship Autonomous Vehicle Systems, Technical University of Munich, 85748 Garching, Germany

[3]Munich Institute of Robotics and Machine Intelligence, Technical University of Munich, 85748 Garching, Germany

CORRESPONDING AUTHOR: R. TRAUTH (e-mail: rainer.trauth@tum.de)

This work was supported by the Technical University of Munich through the Bavarian Research Foundation (BFS).

ABSTRACT Autonomous vehicles face numerous challenges to ensure safe operation in unpredictable and hazardous conditions. The autonomous driving environment is characterized by high uncertainty, especially in occluded areas with limited information about the surrounding obstacles. This work aims to provide a trajectory planner to solve these unsafe environments. The work proposes an approach combining a visibility model, contextual environmental information, and behavioral planning algorithms to predict the likelihood of occlusions and collision probabilities. Ultimately, this allows us to estimate the potential harm from collisions with pedestrians in occluded situations. The primary goal of our proposed approach is to minimize the risk of hitting pedestrians and to establish a predefined, adjustable maximum level of harm. We show several practical applications for informing a sampling-based trajectory planner about occluded areas to increase safety. In addition, to respond to possible high-risk situations, we introduce an adjustable threshold that governs the vehicle's speed when encountering uncertain situations and strategies to maximize the vehicle's visible area. In implementing our novel methodology, we analyzed several real-world scenarios in a simulation environment. Our results indicate that combining occlusion-aware trajectory planning algorithms and harm estimation significantly influences vehicle driving behavior, especially in risky situations. The code used in this research is publicly available as open-source software and can be accessed at the following link: https://github.com/TUM-AVS/Frenetix-Motion-Planner.

INDEX TERMS Autonomous vehicles, collision avoidance, trajectory planning, vehicle safety.

I. INTRODUCTION

AUTONOMOUS driving has gained significant attention in recent years due to its potential to revolutionize the transportation industry. However, achieving fully autonomous driving in dynamic environments remains challenging, as autonomous vehicles must navigate safely and efficiently with unpredictable and dynamic obstacles. Safety depends strongly on the environment in which the vehicle is operating. The vehicle's environment is influenced by uncertainties, which the vehicle must consider when calculating the trajectory. Uncertainties can be very diverse. One of the most significant uncertainties in trajectory planning comes from occluded areas.

These are areas where the vehicle has no complete information about the scenario and dynamic obstacles at the time of trajectory selection. These occlusions can occur for various reasons, e.g., physical objects such as buildings, walls, fences, or other vehicles can obstruct the view of specific areas on the street. Figure 1 shows an example of the hazardous and occluded spots behind parked vehicles while selecting the autonomous vehicle's trajectory. Occluded areas can impact safety, visibility, and, therefore, the overall functioning of autonomous vehicles, especially for unprotected road users like pedestrians or

The review of this article was arranged by Associate Editor Hongkai Yu.

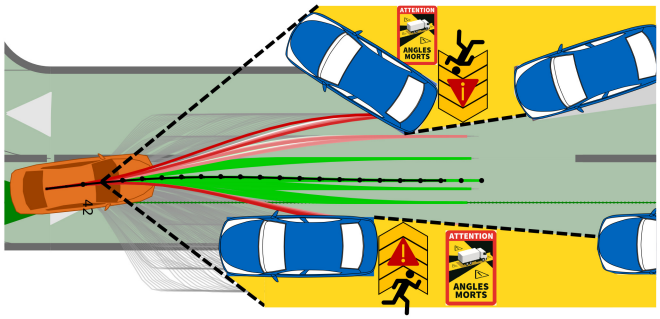

FIGURE 1. Exemplary illustration of hazardous situations in autonomous vehicle trajectory selection.

cyclists who deserve the utmost protection and attention. The trajectory planning algorithm must deal with uncertainties and unknowns that may arise due to perception, prediction, or semantic weaknesses. Several factors influence the visibility of obstacles during driving:

1) Static and dynamic obstacles: e.g., buildings, vegetation, other vehicles, pedestrians, animals, construction, temporary signs.
2) Sensor limitations and weather conditions: e.g., rain, fog, snow, shadows, night, field of view, resolution, reflections, sensor malfunction.
3) Road features and time factors: e.g., curves, hills, tunnels, traffic variations, and events such as demonstrations.

These factors should influence the trajectory choice, e.g., slow down, change lanes, or increase the distance to the side of the road for better visibility. If these factors are not considered, the autonomous vehicle will drive at the target speed (maximum legal speed) on the direct path to the target area without considering the hazards. The general traffic statistics validate the occurrence of severe accidents resulting in personal injuries, particularly in blind spots [1]. Inattentive pedestrians pose a significant risk when crossing roads. Autonomous vehicles must consider these potential hazards, irrespective of culpability. Imagine the following situation illustrated in Figure 1: A vehicle is driving through a narrow road with parked vehicles at the roadside. Some cars are parked in the second row and completely occlude the road's edge. Crossing pedestrians, bicyclists, or vehicles poses a high risk to all road users. At the same time, autonomous vehicles are expected not to impede moving traffic and to reach their destination as quickly as possible. Human drivers assess the risk through occluded areas with their driving experience and by smart situational judgment. The following questions arise: How fast can an autonomous vehicle drive past these parked vehicles? What is the maximum possible harm if the autonomous vehicle misjudges the hazard and fails to brake? Humans accept a residual risk during the decision process [2]. However, the autonomous vehicle needs a model that processes the appropriate information to make safe decisions in situations where occluded areas are present. This requires in-time decision-making, often with safety-critical components. Such fast reactivity to events can only be processed "at the edge" partly based on incomplete and uncertain knowledge. This paper addresses the issues raised and provides a solution on how autonomous vehicles should behave in occluded and hazardous situations. The aim is not merely to safeguard the vehicle but to put it into practice without stopping it in every edge-case situation. In summary, this work presents three main contributions:

1) We present a comprehensive demonstration of how to effectively extract, model, and incorporate information regarding occluded areas, thereby contributing to the mitigation of potential risks.
2) We present a method for a sampling-based trajectory planner that allows the vehicle to deal with occluded areas based on phantom pedestrian estimates.
3) We introduce a metric for calculating the worst-case harm in the event of a collision with crossing pedestrians and show how to adjust driving behavior to a specified harm limit.

II. RELATED WORK

Occlusion-aware trajectory planning has emerged as a prominent research field, attracting significant attention due to its wide-ranging applications in robotics, autonomous driving, and surveillance systems. This section will provide an overview of recent advancements in this area.

Maximum risk calculation: One line of research focuses on assessing the risk associated with crossing pedestrians to minimize potential damage [3], [4], [5], [6], [7], [8]. Several publications have explored this topic, incorporating contextual information as prior knowledge to evaluate the risk of occluded areas. Additionally, considering factors such as comfort, these studies address the vehicle's limitations from the controller's perspective. Some occlusion-aware motion planners have demonstrated collision-free behavior in self-defined edge-case scenarios [9]. Another approach involves the development of a probabilistic risk assessment algorithm for autonomous driving in the presence of occluded areas [10], [11]. The primary objective of this algorithm is to reduce collision rates and enhance driving comfort by assessing risks and improving safety in urban environments.

Partially observable Markov decision processes (POMDPs): POMDPs have been used in various papers to handle occluded areas [12], [13], [14], [15], [16], [17], [18]. These papers leverage POMDP-based behavioral planners to tackle complex scenarios involving occluded areas. Additionally, contextual appearance probability is used to support these algorithms. Some researchers have introduced phantom vehicles and pedestrians to evaluate hazards in challenging situations effectively [12], [13], [14]. Hierarchical decision-making methods have been proposed to support decision-making in specific situations, particularly at intersections [17], [19]. Their framework employs a

higher-level candidate path selector and a lower-level POMDP planner to aid vehicle navigation.

Formal methods and reachable sets: Integration of reachability analysis is another strategy for addressing hazardous situations. In set-based prediction, the reachability analysis calculates all future behaviors of other road users according to the assumptions made [20], [21]. Occluded areas can also be integrated into the set-based prediction assumptions [22], [23]. The set-based prediction approach promises to generalize arbitrary traffic situations and not just represent individual scenarios [22], [24]. Some approaches can be combined with phantom objects to enhance the safety of all traffic participants [22]. Nager et al. [25] even use reachable sets analysis to guarantee passive safety for autonomous vehicles despite occlusions. Another paper proposes a motion planning method for autonomous valet parking in environments with limited visibility [26]. The method utilizes reachable set estimation to account for obstacles and enable safe vehicle movements. It addresses constraints on vehicle motion and uses sensor data to estimate the reachable space around the vehicle. The proposed approach aims to ensure collision-free parking maneuvers.

New concepts and planning extensions: There is also work developing a new planning concept for the problem of occluded areas, for example, using game theory [27]. Zhang et al. formulate the problem as a dynamic zero-sum game between the autonomous vehicle and an initially occluded road user. It derives optimal strategies for both players and sets of initial conditions to avoid collisions. Based on these results, a trajectory planning framework provides worst-case safety guarantees while minimizing conservatism. Collision risk can also be reduced through algorithmic improvements such as maximizing visibility through dynamic lateral position adjustment [28], [29]. The approach aims to optimize the lateral position of the vehicle to improve its perception of the environment and enhance safe and efficient motion planning. The method incorporates a cost function that quantifies the visibility of occluded areas, which is used in the motion planning algorithm to generate optimal trajectories that prioritize improved visibility. There are also extensions for complex edge cases in occlusion-aware trajectory planning. A left turn maneuver represents a unique challenge for the vehicle and is therefore considered separately in another publication [30]. Urban scenarios are especially in focus due to the lack of visibility. The left turn maneuver and successful merging into traffic using a tracked object-based environment representation and object-free sensor fusion, including calculating unobservable regions in a digital map, have already been studied [31], [32]. Furthermore, point clouds generated by a lidar can create a comprehensive obstacle map [33], [34], [35]. By establishing boundaries around these static obstacles, it is possible to accurately predict the potential positions of pedestrians. Leveraging this information, longitudinal motion planners effectively determine target states, enabling proactive measures to avoid any unavoidable collisions with pedestrians who might be obscured in certain areas.

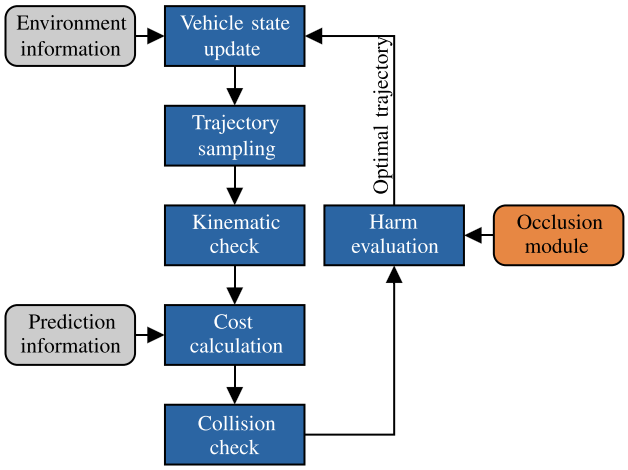

FIGURE 2. Trajectory planning procedure.

III. METHODOLOGY

In the following section, we briefly review the basic architecture of our trajectory planning algorithm and present the novel extensions in order to enable occlusion-aware planning. On the one hand, this entails the comprehensive assessment of high-risk zones. On the other hand, it encompasses a meticulous examination of the potential impact in the unfortunate event of a collision with crossing pedestrians.

A. SAMPLE-BASED TRAJECTORY PLANNING

Our algorithm for considering the hazards of occluded areas is limited to the planning and prediction domains in autonomous driving. The trajectory planning algorithm approach consists of six main steps, illustrated in Figure 2.

The vehicle uses the environmental information to orient itself in the Frenet coordinate system. The trajectory planning algorithm generates several samples in a pre-specified discretization scheme that are checked for validity and ranked according to defined criteria [36], [37]. The generated trajectories are first examined according to kinematic and dynamic single-track model criteria, ensuring the selected trajectory is drivable and does not exceed the vehicle's dynamic driving limits. Afterward, the feasible trajectories can be evaluated using defined cost functions. The prediction information is used to consider dynamic objects' occupancy, which is done using a neural network [38]. Collision probabilities can be added to the cost of the trajectory planning algorithm via a weighting factor. The total cost function is evaluated for all valid trajectories, considering both collision costs and comfort and time consumption costs. For computational time reasons, the lowest-cost trajectories are examined for collisions afterward. Trajectories that result in a safe collision with static objects or lane boundaries are set to invalid. This is also true for quasi-static objects, which hardly change their position to the ego movement.

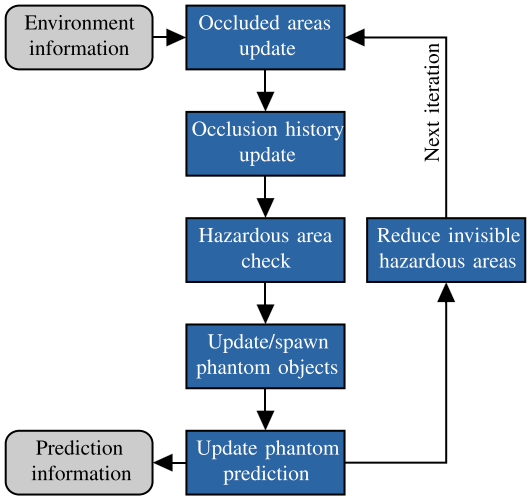

FIGURE 3. Occlusion module procedure.

The new approach from this paper is that before the optimal trajectory is selected, the information from the new occlusion module is used to estimate the potential hazard based on various calculations. In addition to the standard trajectory assessment performed in the application scenario, an additional assessment of potential harm and damage related to crossing pedestrians is performed.

B. OCCLUDED AREAS AND PHANTOM PEDESTRIAN PREDICTION

The following section outlines how pedestrians are handled in our trajectory planning process. The occluded areas contain more information not considered in the standard trajectory planning algorithm. Therefore, our new occlusion module is introduced to calculate this information and provide it for the trajectory planner. The process for considering occluded areas can be seen in Figure 3.

Occluded areas update: The calculation of occluded areas involves an advanced sensor model that leverages geometric and semantic data to determine occluded areas.[1] This process utilizes environmental information to calculate the polygons representing the occluded areas accurately. Furthermore, the sensor model undergoes regular updates at each iteration step to ensure its reliability and precision. The visible area A_{va} in Equation (1) is the set difference between the occluded area behind boundaries and obstacles A_{oa} and the intersection between the area of the sensor radius A_{sr} and the area of the lanelet network A_{ln} unified with a defined buffer zone A_{bz}.

$$A_{va} = (A_{sr} \cap (A_{ln} \cup A_{bz})) \setminus A_{oa} \tag{1}$$

An illustrative distinction between visible and occluded areas can be found in Figure 4. The green area represents the visible area, the red area represents the occluded area, and the yellow area represents the previously unseen area.

1. https://pypi.org/project/commonroad-helper-functions/

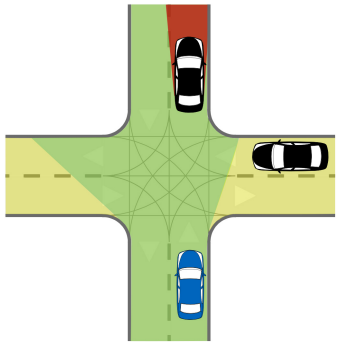

FIGURE 4. Occluded area calculation. Green is the visible area. Red is the occluded area. Yellow is the unknown area.

Update occlusion history: The visible A_{va} and occluded areas A_{oa} are discretized for better differentiation. The discretizations hold a history so that past time steps can be considered for the uncertainty calculations. The uncertainty map is created by analyzing the time history of visible and occluded areas. This is done by tracking the discretized points $T_{A_{oa}}$ and checking how long a point has not been visible. The information about visible and occluded points and their history can then be used for cost evaluation. The increase occurs up to a threshold value that can be defined. After this threshold, a discretization point is treated as unknown if it had never been visible before, like in Equation (2).

$$\alpha_i = \begin{cases} visible & \exists \alpha \in A_{va} : T = 0 \\ occluded & \exists \alpha \in A_{oa} : 0 < T < t_{max} \\ unknown & \exists \alpha \in A_{oa} : t_{max} < T \end{cases} \tag{2}$$

Checking hazardous areas: The occluded areas are analyzed to identify possible hazardous areas and, thus, possible spawn points for phantom pedestrians. These areas, such as behind parked cars on the side of the road, are hazardous for crossing pedestrians. This is achieved by analyzing the objects in the environment in the context of the semantic map information and the tracked area points in Equation (2). To do this, occluded areas must reach a minimum size so that there is a geometric possibility that a pedestrian can step out of an occluded area in the ego vehicle driving direction.

Update/spawn phantom objects: The process of generating phantom objects involves well-defined steps to enhance realism. Initially, spawn points are determined by identifying parked vehicles or other static obstacles that obstruct the view of the ego vehicle. To accomplish this, relevant static objects are carefully selected, focusing on those in the direction of travel and sorted based on their distance from the ego vehicle. A search is then conducted to identify potential object candidates for a spawning area behind them. It is essential to consider a buffer zone around these objects, as pedestrians tend to maintain a certain distance from them. This offset is crucial because pedestrians are not mere dimensionless points but possess a definite width. Once the corner points of the buffer zone of the obstacles are detected,

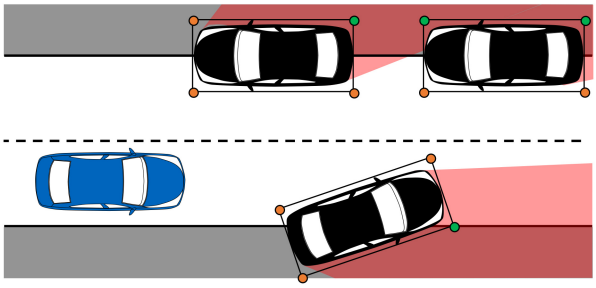

FIGURE 5. Spawn point detection illustration. Visible corner points VCPs are illustrated in orange and non-visible corner points in green.

they undergo evaluation, and suitable spawn areas are chosen. For each potential spawn point, the method determines one point towards the reference path (TRP) and another point in the opposite direction (OPP). These auxiliary points are used to evaluate the actual spawn points. Figure 5 shows the parking obstacles and their visible corner points (VCP) as well as the non-visible corner point (nVCP). The obstacles are simulated as oriented bounding box (OBB) [39].

Furthermore, specific selection criteria are applied to determine whether an area behind an object qualifies as a candidate spawning area:

1) OPP is not in the visible area.
2) OPP is not in the obstacle.
3) OPP is within the scenario.
4) TRP is not in the obstacle.
5) Phantom pedestrian shape does not intersect another obstacle.

A selection method ensures the accuracy of identifying spawn points for phantom objects. This method considers the spawn point's proximity to the ego vehicle and its distance from the reference path. It guarantees that only a single spawn point is assigned to each static obstacle, optimizing the entire process. The initialized phantom objects are oriented to move orthogonally to the ego vehicle's reference path direction to create a worst-case situation.

Update phantom predictions: The phantom objects are assigned generated predictions updated at each time step. The prediction is straight across the roadway, orthogonal to the vehicle direction. The Frenet planning algorithm can use the artificially generated trajectory to adapt the driving behavior to the risk of the situation. The worst-case situation is assumed in each time step.

Reduce occluded hazardous areas: The vehicle's field of view can be actively expanded, offering increased safety by reducing hazardous areas. Adjusting the lateral distance of the vehicle to the reference path directly impacts the visible area. To perform a preliminary simulation, the endpoints of the sampled trajectories can be used. The visibility of the trajectory pattern endpoints is assessed, taking into account only objects that are currently visible and predictable. The evaluation method distinguishes between various types of areas, allowing for the assignment of different weights to visible and occluded areas. Additionally, it enables the differentiation of sidewalks, regular road sections, and prioritized road sections along the reference path.

C. COLLISION PROBABILITY AND PEDESTRIAN HARM ESTIMATION

When considering autonomous driving, we can define maximum risk as the combination of two essential factors: the likelihood of a collision (p) and the potential harm resulting from such a collision (H) through a selected trajectory $\mathcal{T}$ [40], [41].

$$R(\mathcal{T}) = \max(p(\mathcal{T})H(\mathcal{T})) \tag{3}$$

Various uncertainties, perceptions, or vehicle control influence the collision probability in autonomous driving. We focus on the collision probabilities of predicting other road users' movements.

Below, we will define the term *harm* and present a set of metrics developed to measure it. The phantom pedestrian prediction method will be utilized to estimate the potential harm caused by the failure to observe occluded areas. According to the definition provided in [42], harm can be understood as a negative consequence that causes physical or other injury or damage to individuals or entities. It's important to note that in this context, the primary focus is on harm to human beings. Throughout the following discussion, any damage or impairment to human health will be considered harmful. This is consistent with legislative priorities, which give precedence to the protection of human life over property or animal welfare [43].

When assessing the severity of traffic-related injuries, a widely used measure is the Abbreviated Injury Scale (AIS). The AIS was first introduced in 1969 as part of the General Motors Collision Performance and Injury Report [44], featuring fewer than 75 injury codes. Over time, it has been expanded to include roughly 2,000 injury codes with corresponding AIS scores. In cases where a person sustains multiple injuries, their overall AIS score - known as the Maximum AIS (MAIS) - is determined by the highest individual AIS score. Although in-depth crash databases can provide detailed information on multiple injuries sustained by an occupant, police-reported datasets usually only include the Maximum AIS (MAIS) score for each person. The levels of AIS scores and related injuries are displayed in Table 1.

In addition to the protection of the road user, other factors describe the accident's severity. The resulting equations (4) and (5) help us to understand the harm that occurs during a collision, taking into account factors such as mass (m), speed (v), collision angle (α), and empirically determined coefficients (c_0, c_1, c_{area}) [40].

$$\Delta v_A = \frac{m_B}{m_A + m_B}\sqrt{v_A^2 + v_B^2 - 2v_A v_B cos\alpha} \tag{4}$$

$$H = \frac{1}{1 + e^{c_0 - c_1 \Delta v - c_{area}}} \tag{5}$$

To assess the severity of the harm on a scale from 0 to 1, we utilize the probability of an accident with MAIS3+

TABLE 1. AIS scores of injury types.

AIS score	Level of severity	Description
0	No injury	Not injured
1	Minor	Superficial
2	Moderate	Reversible injuries
3	Serious	Reversible injuries
4	Severe	Life-threatening
5	Critical	Non-reversible injury
6	Fatal	Virtually not survivable
9	Unknown	Unknown severity

severity based on the Abbreviated Injury Scale [45]. This means that we calculate a probability that at least one accident of severity class 3 or higher will occur.

The resulting harm from a potential collision is determined using the National Highway Traffic Safety Administration's Crash Report [40], [41]. In the following, we introduce logistic regression, a statistical technique, to analyze the discrete dependent injury variable Y to distinguish between different road users and determine the crash's severity. This variable can take on two or more values. The independent variables x can be either discrete or continuous. The logistic regression formula produces an S-shaped curve, representing the probability that the event $Y = 1$ occurs [46]. The outcome $P(Y|X)$ will vary between 0 and 1 for a vector of independent variables x_j. Equation (6) provides the corresponding formula for the regression model:

$$P\big(Y = 1|X = x_j\big) = \frac{1}{1 + e^{-(\beta_0 + \sum_{i=1}^{n} \beta_i x_{i,j})}} \tag{6}$$

The model typically incorporates a constant β_0 and coefficients β_i for n input variables, combined in the vector β. The probability of Y being 1 is often denoted as $\pi(X)$. Similarly, the probability of Y being 0 can be expressed as the complementary event:

$$P\big(Y = 0|X = x_j\big) = 1 - \pi(X) \tag{7}$$

The harm score is particularly interesting when considering vulnerable groups, as a collision with unprotected road users significantly impacts harm more than protected road users. The functionality of the harm function can be taken from [40], [47].

D. HARM EVALUATION

The information from the occlusion module is subsequently utilized to finely tune and enhance the driving behavior of the trajectory planner, as depicted in the last step of Figure 2. In addition to passive uncertainty assessment information, this information can also be used to adjust trajectory selection. Equation (8) shows how the harm risk costs can be added to the standard cost function with the weighting factor ω.

$$J_{sum}\big(\zeta|f_\zeta\big) = J_1(\zeta)\omega_1 + J_2(\zeta)\omega_2 + \cdots + J_H(\zeta)\omega_H \tag{8}$$

where J_{sum} is the total cost of the trajectory $\zeta \in \mathcal{T}$ when the kinematic feasibility f_ζ is satisfied. As with all analytical models, the weighting factor ω must be chosen carefully. Previous work has investigated how to find weights in specific domains [48] or how to derive weights with supervised learning from, for example, human data [49]. The weighting factor ω linearly affects the trajectory selection decision. However, the cost functions are non-linear, so they have a more significant impact on the result depending on the situation. Estimating the weighting factors is sufficient to demonstrate the algorithm's functionality. Due to the non-linear relationship of the collision probability, the harm costs increase sharply when a collision is imminent. However, the harm value can also be used as a validity check. Trajectories above the maximum allowed harm value H_{max} are declared invalid. The procedure can be taken from Equation (9).

$$v_\zeta = \begin{cases} valid & \exists \zeta \in \mathcal{T} : H(\zeta) \leq H_{max} \\ invalid & H(\zeta) > H_{max} \end{cases} \tag{9}$$

Suppose no trajectories are available below the specified harm value. In that case, the kinematically feasible trajectory with the lowest future harm value (stopping trajectory) is selected until the harm value falls below the threshold. This is especially not the case if the planning horizon is set long enough because the vehicle has more time to react in advance.

IV. RESULTS AND ANALYSIS

The following analysis shows the simulation environment and the scenarios illustrating how the method works. Subsequently, the influence of the method is shown by the cost function and the influence of a maximum harm value on the driving behavior of the vehicle. We will also investigate other aspects, such as computation time.

A. SIMULATION ENVIRONMENT AND SCENARIOS

Ensuring the effectiveness of developed modules in addressing occluded areas in autonomous driving heavily relies on identifying pertinent test scenarios. Therefore, we will comprehensively evaluate 2019 to 2022 data from the reputable Federal Statistical Office [1]. Our focus will specifically revolve around accidents that have resulted in personal injuries. On average, it can be inferred that 70 % of accidents involving personal injury occur within the city. Furthermore, despite passenger cars covering significantly greater distances on average, it is crucial to acknowledge that a substantial 45 % of all injuries involve vulnerable road users such as cyclists, motorcyclists, and pedestrians [50, p. 100]. Among vulnerable road users, pedestrians constitute a significant portion affected by traffic accidents. Approximately 25 % of such incidents resulting in personal injuries are attributable to excessive speed or inadequate distance. Another 30 % can be traced back to errors made while turning, entering, exiting, or disregarding the right of way. In urban areas, it is reasonable to assume that these factors and improper conduct towards pedestrians often contribute to accidents occurring. Many accidents can be attributed to pedestrians carelessly crossing the road. More than half of

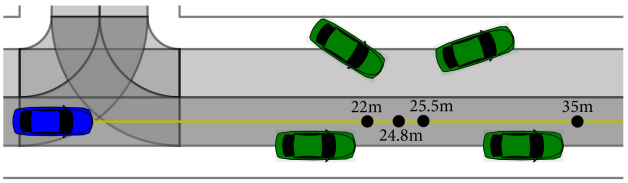

FIGURE 6. Scenario 1: Narrow street with parked vehicles on the ego-drive and the opposite side of the drive.

the causes behind these accidents stem from crossing without being mindful of vehicular traffic. Additionally, nearly 20 % of accidents occur when pedestrians unexpectedly emerge from obscured sightlines [51, p. 17]. The statistical evaluation from Germany largely corresponds to the evaluation in the United States in urban areas [52], [53]. Four different scenarios are created based on accident statistics to illustrate the functionality of the proposed algorithm. In addition to overtaking parked vehicles, turning maneuvers are also examined. Particular attention is paid to the narrowing of the road, which restricts the vehicle's field of vision. We use a 2D simulation environment to evaluate our algorithm approach in edge-case crossing pedestrian scenarios [54]. The Figures 6, 9, 12 and 13 showcase exemplary scenarios including parked vehicles. The parked vehicles in the scenarios are placed so that occluded areas arise. First, the driving behavior is described qualitatively. In addition, the influence on the harm level is analyzed, which should provide information about the hazardous situation of a crossing pedestrian.

B. HARM COST-TERM EVALUATION

In this subsection, the impact of phantom object prediction on driving behavior is investigated via the cost function of the sampling-based trajectory planning algorithm. Scenario 1 (Figure 6) is initialized with a target speed of $12\,\mathrm{m\,s^{-1}}$.

We investigate different weighting factors to examine the influence on driving behavior. Figure 7 illustrates the velocity profile over the s-coordinate in Scenario 1. The dashed lines show the positions where the phantom objects are created. Initially, a speed reduction can be observed in all configurations due to the collision avoidance maneuver. The ego vehicle has to drive to the left in the direction of the center of the lane to pass the first obstacle. It can be observed that the higher weighting of the collision probability with the phantom objects leads to a reduced vehicle speed compared to the standard trajectory planning algorithm.

Once the hazardous points have been passed, the vehicle accelerates linearly to the target speed, regardless of the weighting factor. The speed adaptation affects the potential harm that can occur to crossing pedestrians. The effects can be seen in Figure 8. The standard trajectory planning algorithm poses a potential risk of serious harm, whereas the occlusion module mitigates it to a more superficial impact. The following will examine how the standard

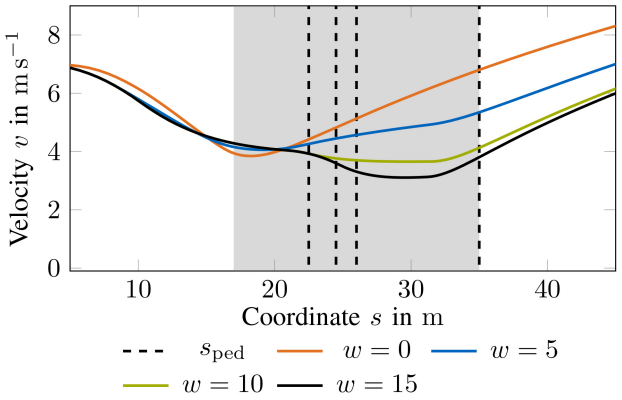

FIGURE 7. Scenario 1: Velocity profile of runs with different phantom prediction cost weights.

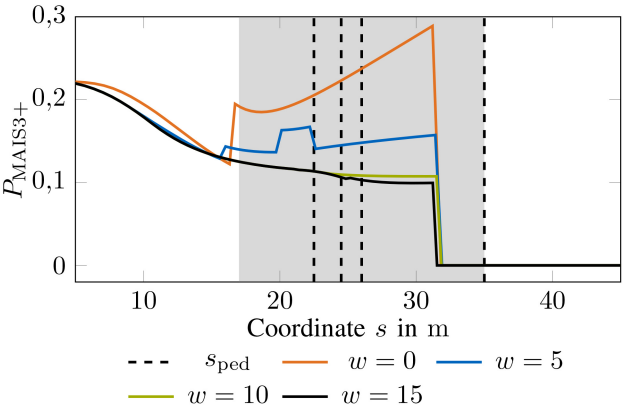

FIGURE 8. Scenario 1: Pedestrian harm of runs with different phantom prediction cost weights.

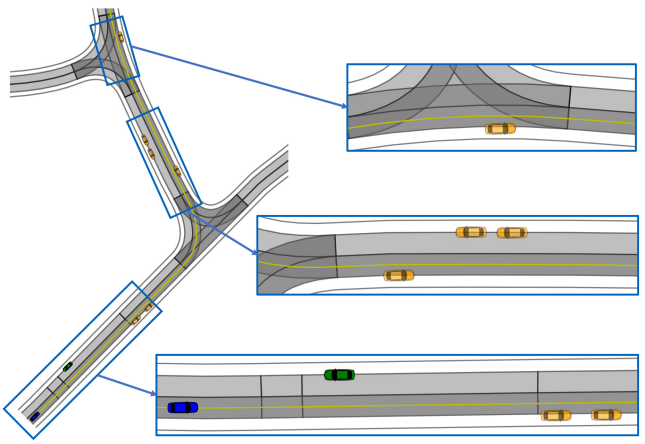

FIGURE 9. Scenario 2: Complex scenario with several occluded areas.

trajectory planner performs compared to the occlusion-informed trajectory planner when a pedestrian crosses the street. In this case, we simulate an actual pedestrian who causes a collision when overlapping with the vehicle. The vehicle can make an emergency stop from the moment of visibility. Table 2 shows the example scenarios with different scene setups. s_{ped} represents the occluded position where

TABLE 2. Collision and harm table for specified scenarios.

No.	s_{ped}	s_{ego}	weights	collision speed	$P_{\text{MAIS3+}}$
1	22 m	9 m	$w = 0$	$2.24\,\text{m}\,\text{s}^{-1}$	7.5 %
			$w = 15$	**no coll.**	**no coll.**
1	35 m	25 m	$w = 0$	$5.38\,\text{m}\,\text{s}^{-1}$	15.7 %
			$w = 15$	**no coll.**	**no coll.**
2	91 m	68 m	$w = 0$	$7.71\,\text{m}\,\text{s}^{-1}$	25.8 %
			$w = 15$	**no coll.**	**no coll.**
2	91 m	69 m	$w = 0$	$8.06\,\text{m}\,\text{s}^{-1}$	27.7 %
			$w = 15$	$3.14\,\text{m}\,\text{s}^{-1}$	9.5 %
2	91 m	71 m	$w = 0$	$8.88\,\text{m}\,\text{s}^{-1}$	32.2 %
			$w = 15$	$2.88\,\text{m}\,\text{s}^{-1}$	8.9 %
2	167 m	150 m	$w = 0$	$10.53\,\text{m}\,\text{s}^{-1}$	42.4 %
			$w = 15$	**no coll.**	**no coll.**
3	42 m	33 m	$w = 0$	$6.63\,\text{m}\,\text{s}^{-1}$	20.6 %
			$w = 15$	$1.10\,\text{m}\,\text{s}^{-1}$	6.0 %
4	82 m	62 m	$w = 0$	$6.44\,\text{m}\,\text{s}^{-1}$	19.1 %
			$w = 15$	**no coll.**	**no coll.**
4	114 m	102 m	$w = 0$	$11.06\,\text{m}\,\text{s}^{-1}$	47.3 %
			$w = 15$	**no coll.**	**no coll.**

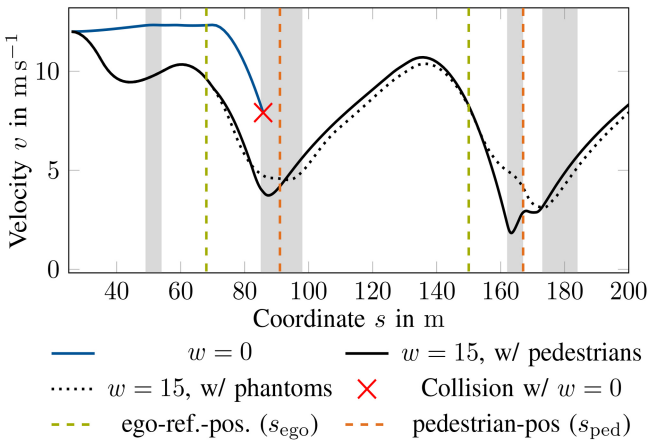

FIGURE 10. Scenario 2: Speed profile of actual crossing pedestrians.

the pedestrian crosses the street. s_{ego} is the position of the ego vehicle when the pedestrian crossing the street is initialized.

Figure 10 illustrates a run with $s_{\text{ego}} = 68\,\text{m}$ in Scenario 2 in Table 2. It can be observed that the vehicle drives faster without considering the occluded areas and causes strong collisions with the crossing pedestrians in all situations. Our proposed method effectively reduces the vehicle's speed promptly, aligning it with the risk of collision with phantom objects. Subsequently, upon the emergence of a real pedestrian, the vehicle further decreases its speed to ensure safety. Once the blind situation is surpassed, the vehicle resumes following the speed set by the occlusion-aware module. The possible harm $P_{\text{MAIS3+}}$ resulting from the driving behavior can be seen in Figure 11. Different weights of harm prioritization are shown.

It also illustrates how much the high prioritization ($w = 15$) deviates in percentage from the standard trajectory planning algorithm ($w = 0$). A several times higher risk is taken before hazardous situations without considering the occluded areas. If crossing pedestrian objects are simulated, a collision with serious harm occurs despite the braking reaction. On the other hand, the proposed algorithm significantly reduces the harm to a level with light and reversible harm. The harm level can not only be reduced but also adjusted. This means that even in the case of an unavoidable collision, the extent of harm can be reduced to the point where there is no serious danger to the lives of crossing pedestrians. Figure 12 illustrates a scenario of turning right with an extensive non-visible area.

The turning maneuver notably attenuates the vehicle's field of visibility. Accordingly, the vehicle slows significantly when passing the stuck vehicle compared to the standard trajectory planning algorithm. Table 2 gives comprehensive information on potential harm values.

C. MAXIMUM HARM VALIDITY CHECK EVALUATION

In the upcoming studies, we will utilize the calculated harm value to investigate driving behavior while incorporating validity checks. A trajectory is valid when its calculated harm value is below the limit. We have established five distinct harm thresholds that trajectories must not surpass. If no sampled trajectory in one timestep falls below the specified threshold, the model selects the first feasible and valid trajectory with the lowest theoretical harm value. For a trajectory to be considered valid, it must be free from collisions with stationary objects and route boundaries while also being kinematically feasible. Figure 14 shows the harm values of each run in Scenario 4.

It can be determined that the set harm thresholds are not exceeded. However, the other cost functions are decisive for the exhaustion of the threshold since the harm control is in contrast to the time costs of the trajectory planning algorithm. It can also be observed that the lateral distance to the parked objects increases as the harm value is considered. The lower the maximum threshold for harm, the sooner potential harm from hazards is detected. This is because the geometric planning horizon is longer at higher speeds, while the temporal planning horizon remains identical. This also results in a more significant velocity oscillation with a lower allowable harm value. The vehicle may stop in some settings if the maximum harm value is too low. In this case, the sampling of trajectories must be adjusted so that the solution space is large enough to select trajectories that satisfy the low harm value. Achieving travel speed is in target conflict with the harm threshold. Driving behavior is mainly influenced by the vehicle's lateral position in relation to the parked vehicles and the speed of the vehicle in order to stay below the maximum allowable harm value. The influence of the model on driving behavior is examined in the following section.

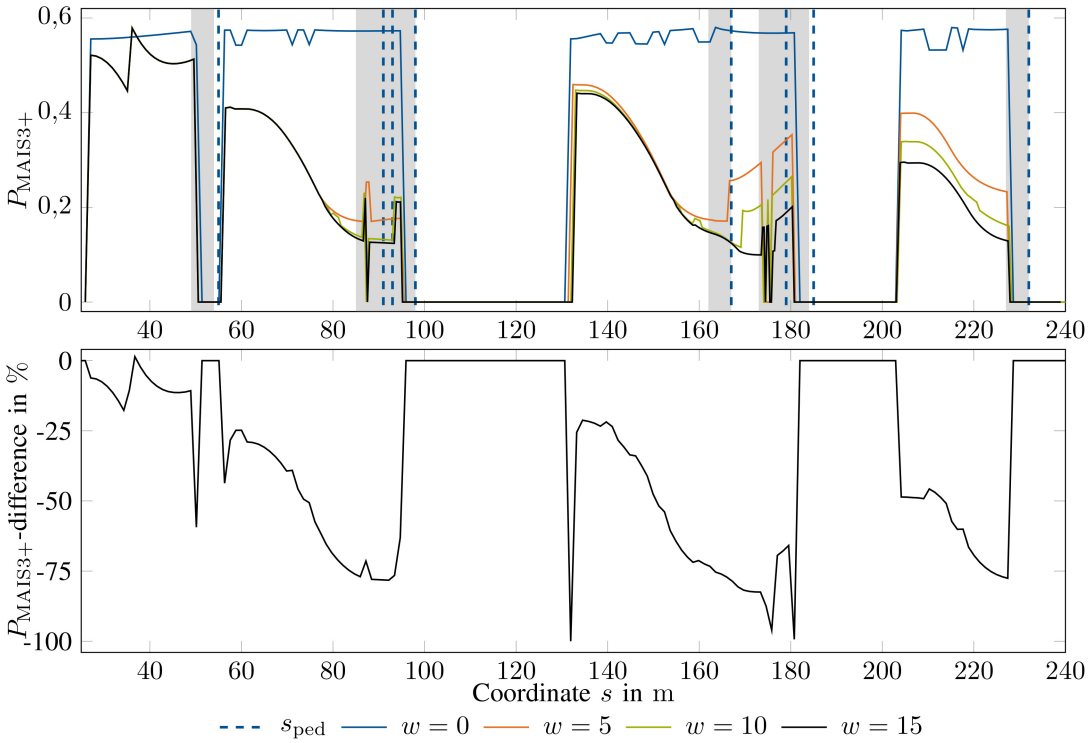

FIGURE 11. Scenario 2: Pedestrian harm in case of a possible collision of the selected trajectory of different simulation runs with cost weights. Below the percentage difference between the runs with $w = 0$ and $w = 15$.

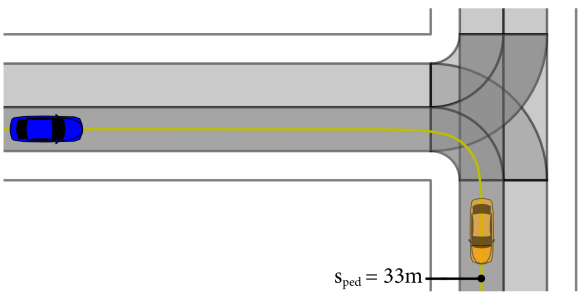

FIGURE 12. Scenario 3: Turning to the right with a stopped vehicle in front.

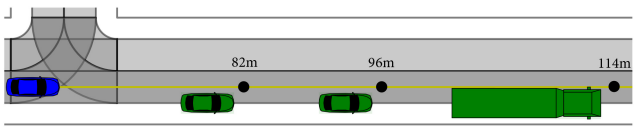

FIGURE 13. Scenario 4: Narrow street with parked vehicles on the ego-driving side.

D. DRIVING BEHAVIOR ADAPTION

The maximum harm limit also changes the driving behavior. Reducing the speed and increasing the distance to the hazardous areas increases travel time. The influence on the travel time to drive from the initialization to the final s-coordinate can be seen in Figure 15. The simulation is run several times with different harm limits. The cost function that increases the visible area (Figure 3) is weighted with different factors w_d to illustrate the functionality and the influence on the algorithm. For clarity, only two runs are shown here. The travel time of the first run with $w_d = 0$ and $P^{max}_{\text{MAIS3+}} = 0$ is 80.8 % higher than without any restrictions. The increase above the value of $P^{max}_{\text{MAIS3+}} = 0.4$ hardly increases the travel speed. This saturation effect depends on the target speed of the vehicle. The higher the target speed, the later the travel speed saturates. The orange line in Figure 15 represents a run with a weighting factor $w_d = 6$. This ensures that the future visibility of hazardous areas is considered when selecting the optimal trajectory. The influence on the lateral deviation to the reference path can be seen in Figure 16. The additional distance from parked vehicles means that occluded areas become visible sooner. This allows the vehicle to achieve a higher overall scenario speed. Speed saturation is reached sooner. The additional lateral deviation leads to a higher travel time with a maximum harm limit of $P^{max}_{\text{MAIS3+}} = 1.0$. The vehicle needs more time to reach its destination due to the longer distance traveled.

The lateral distance to the hazardous non-visible areas can reduce the risk by making them visible earlier. Reducing non-visible hazardous areas (Figure 3) is an essential task of the algorithm to maintain traffic flow because uncertainties can also be reduced. Essentially, the driving behavior can be described by the lateral distance of the vehicle to the reference path. In Scenario 4 (Figure 13), different weightings are analyzed to evaluate trajectories based on the future visibility of occluded areas. Figure 16 shows the different trajectories dependent on the weighting factor w_d. It should be noted that the lateral distance

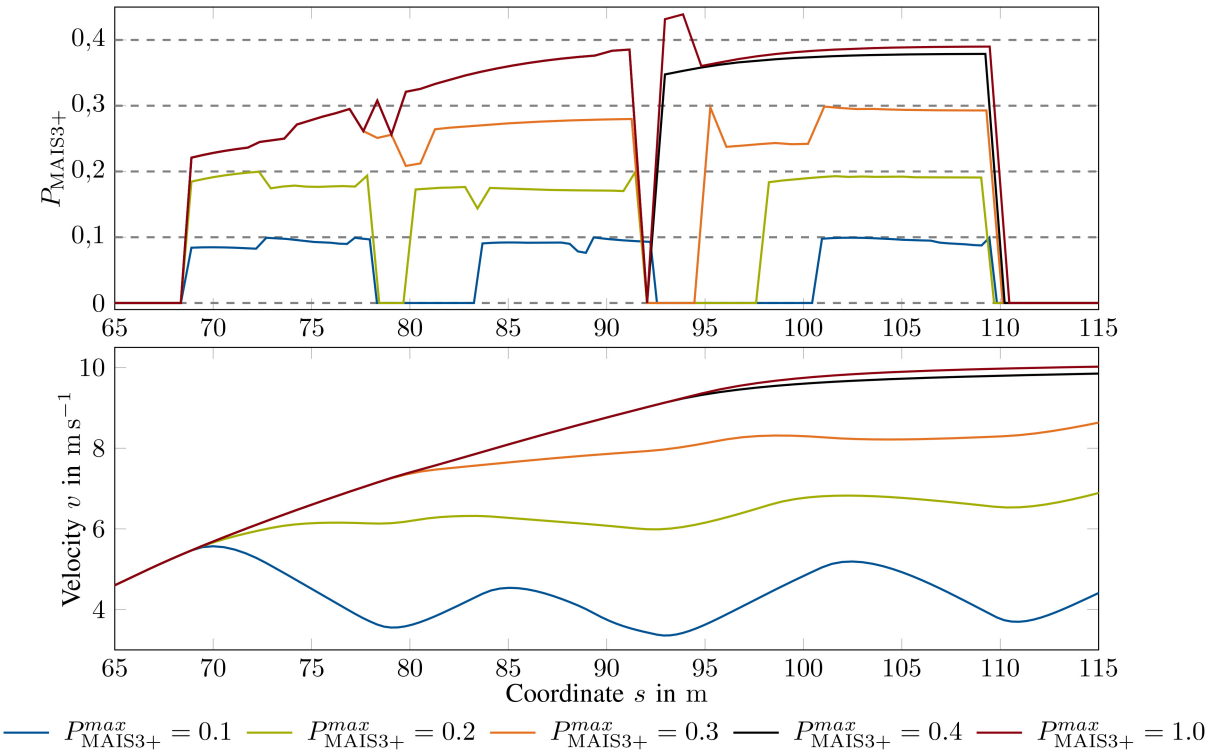

FIGURE 14. Scenario 4: Pedestrian harm in case of a possible collision of the selected trajectory of different simulation runs with validity checks.

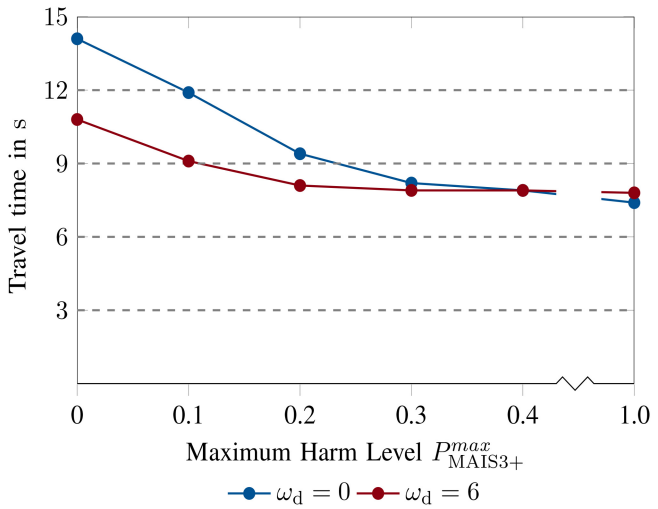

FIGURE 15. Scenario 4: Travel time in seconds s with different additional visible area weight factors $w_d = 0$ and $w_d = 6$.

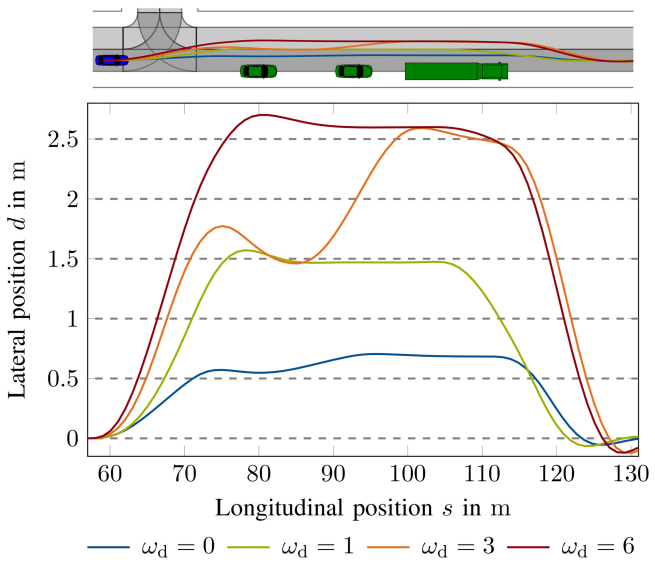

FIGURE 16. Scenario 4: Lateral distance (d-distance) to reference path along longitudinal s-position in m for several runs with different weighting factors w_d.

increases over time before reaching the hazardous areas. This ensures that hazardous areas are visible earlier, allowing for an earlier increase in speed. The blue line represents the minimum distance the vehicle must maintain to avoid collisions with static objects. The adjacent lane limits the maximum allowable lateral distance to the reference path. When a moving vehicle in the other lane approaches our direction, the distance to the parked vehicles is reduced to avoid a collision. As a result, the speed of the vehicle is reduced to keep the risk of possible crossing pedestrians constant in the non-visible area.

E. REAL-TIME CAPABILITY

In the following studies, the real-time capability of the algorithm and the runtime are investigated to demonstrate its real-world applicability. The four scenarios presented are used to investigate the runtime of all parts of the

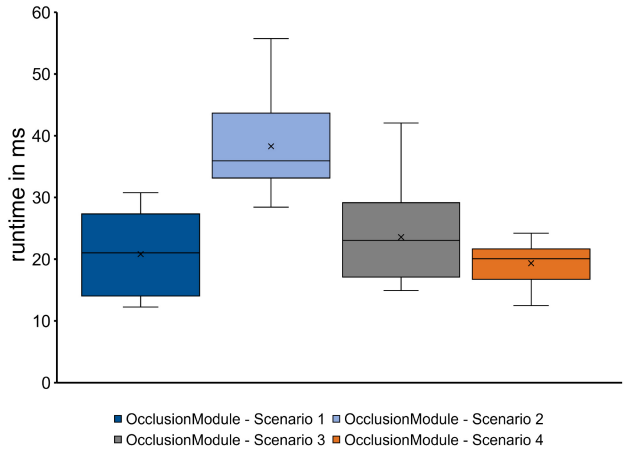

FIGURE 17. Runtime of the Occlusion Module per scenario in milliseconds in boxplot format for one timestep iteration.

presented Occlusion Module in Figure 3. The Python code[2] is executed on the CPU (Intel Core i7-10850H, 16 GB RAM) in the following investigation. Figure 17 shows the boxplot representation of the runtime for each scenario in every iteration. The runtime is represented in milliseconds. The entire module is executed without visualization of the planning functionality. It can be observed that the average execution time is 28.2 milliseconds, and the maximum execution time is 64.58 milliseconds. We calculate 450 trajectories per planning iteration during the run; for larger areas to be calculated, as in Scenario 2, the calculation time may increase briefly. The computation time is generally relatively low, although the code has not been optimized for performance. The average trajectory generation and evaluation runtime is 6.34 milliseconds for all four scenarios. The maximum computation time is 8.79 milliseconds. High performance is achieved through optimized and parallelized C++ code.[3]

V. DISCUSSION

Our simulation results generally indicate the performance and limitations of our proposed occlusion-aware trajectory planning method. We obtain comparable results in the behavior of the autonomous system as obtained in other approaches with different planning systems [55]. The selected edge-case scenarios support the effectiveness of the occlusion-aware trajectory planner by demonstrating reduced risky behavior in occluded areas and driving situations. The results shed light on the potential of using harm metrics related to occluded areas to measure the risk of crossing pedestrians. The sampling-based trajectory planner can adapt the driving behavior flexibly without using pre-determined rule-based methods. The results show that adjusting driving behavior can significantly reduce the potential for harm to pedestrians. The reduction is achieved primarily by strategically reducing speed, choosing a less harmful trajectory, and adjusting overall driving behavior in hazardous situations.

The harm reduction depends mainly on the target speed. Clearly, reducing the target speed can decrease the theoretical harm value; however, this doesn't include the overall hazard potential, and such a reduction could result in a freezing robot problem [56]. The results demonstrate that our approach allows a more dynamic consideration of the hazard at the level of harm to achieve a better pedestrian impact metric. In addition, worst-case information can be better integrated into the trajectory planner's decision-making process, regardless of how the vehicle should ultimately behave and how much risk we can accept [57].

The results indicate that our method frequently prevents pedestrian collisions in occluded areas. When collisions occur, the harm to pedestrians is greatly minimized without stopping the vehicle entirely in a hazardous environment. However, collisions may still occur in high-risk situations, but with significantly less harm. The harm value then depends on the parametrization of the method. In reality, however, such situations are unlikely, so a specific risk is accepted, depending on the setting, to maintain the traffic flow. Importantly, this approach ensures smooth traffic flow without relying on a zero-harm assumption. Instead, it demonstrates the dynamic relationship between driving behavior and harm, emphasizing the importance of context in achieving optimal results. When encountering an actual pedestrian, for example, it can be observed that the vehicle continues to reduce its speed, as shown in Figure 10. This is because the actual pedestrian continues to cross the road, while the phantom object dissipates when a critical situation with sufficient visibility is passed. Figure 15 and 16 illustrate the adjustment of the driving behavior by the model. The lateral adjustment of the position can increase the travel speed at the same harm level, but this is not useful in every driving situation. If other vehicles are parked opposite, as in Scenario 1, or if there is an oncoming vehicle, the risk would increase further. However, unfavorable behavior in such situations can be excluded due to the prediction algorithm used [38].

In addition, by introducing validity checks for compliance with a maximum harm value, we could provide an effective method to set the harm limit independently of the maximum speed limit. The technical implementation of the harm limit could allow legislators to set a harm threshold in difficult and poorly visible situations where a residual risk remains. Which weightings and settings are the best still needs to be evaluated. How to adjust cost parameters in general has been explored in other work [48], [49]. The setting of these parameters generally depends highly on the system architecture of the analytical models. In addition, legislators, ethicists, and ergonomists must specify the desired driving behavior.

The results specifically focus on the uncertainties at the prediction and planning stages. Given the study's methodology, we haven't considered additional uncertainties

2. https://github.com/TUM-AVS/Frenetix-Motion-Planner
3. https://github.com/TUM-AVS/Frenetix

such as sensor noise, road friction coefficients, or controller inaccuracies. While we haven't factored in uncertainties like perception [27], it's worth mentioning that our method primarily deals with static obstacles that limit the field of view, typically identified reliably by perception systems. The method works for occluded areas behind clearly visible static obstacles and given semantic information. The current implementation can only partially cover noise, object uncertainties, and other incomplete information in the map area. Additionally, the planning concept and the set planning horizon influence the assessed risks of the model. The longer the planning horizon, the earlier risks are identified. However, this corresponds to all the other problems that can arise when using a planning horizon.

VI. CONCLUSION & OUTLOOK

In this paper, we presented a comprehensive multi-stage trajectory planning approach that addresses the crucial aspects of adapting vehicle driving behavior in occluded areas. This research aims to respond to hazardous situations caused by occluded areas according to the potential harm value. In this context, we enhanced a given sample-based trajectory planner with a newly developed occlusion model. We employ a systematic evaluation process that leverages semantic map information and object data over time to identify potential hazardous zones within occluded areas. Using phantom objects with prediction information can effectively map worst-case scenarios, providing valuable insights into collision probabilities involving crossing pedestrians. Our trajectory planner can effectively adapt to this situation and select a safer and slower trajectory. With this change in the trajectory, the potential harm to crossing pedestrians can be significantly reduced. Harm consideration is incorporated by weighting the cost function based on the generated trajectories. In addition to including the reduction of harm in a potential collision, our method prioritizes maintaining traffic flow and mitigating potential issues with stagnant or freezing autonomous vehicles. Further studies are needed to determine the appropriate level of harm in a given situation or to more accurately evaluate the acceptability of potential harm when navigating through occluded areas. In addition, future studies need to investigate the potential impact of incorporating sensor uncertainties, state estimation, and road user prediction into our presented method. How the model behaves in the presence of incomplete information, such as missing semantic map information, could also be investigated. Future research may examine the specifics of occlusion-aware algorithms in diverse international and cultural environments. Significant questions persist regarding the algorithm's adaptability and generalizability, particularly in unique settings like densely populated megacities. Furthermore, the creation of an extensive, standardized dataset focused on occlusion-related scenarios would significantly improve the quality and relevance of future studies.

REFERENCES

[1] S. B. Destatis. "Verkehr: Verkehrsunfälle." 2022. [Online]. Available: https://www.destatis.de/DE/Themen/Gesellschaft-Umwelt/Verkehrsunfaelle/Publikationen/Downloads-Verkehrsunfaelle/verkehrsunfaelle-jahr-2080700217004.pdf

[2] S. Kolekar, J. de Winter, and D. Abbink, "Human-like driving behaviour emerges from a risk-based driver model," *Nat. Commun.*, vol. 11, no. 1, p. 4850, 2020. [Online]. Available: https://doi.org/10.1038/s41467-020-18353-4

[3] M. Koc, E. Yurtsever, K. Redmill, and U. Oezgüner, "Pedestrian emergence estimation and occlusion-aware risk assessment for urban autonomous driving," in *Proc. IEEE Int. Intell. Transp. Safety Conf. (ITSC)*, 2021, pp. 292–297.

[4] M. Schratter, M. Bouton, M. J. Kochenderfer, and D. Watzenig, "Pedestrian collision avoidance system for scenarios with occlusions," in *Proc. IEEE Intell. Veh. Symp. (IV)*, 2019, pp. 1054–1060.

[5] F. Damerow, T. Puphal, Y. Li, and J. Eggert, "Risk-based driver assistance for approaching intersections of limited visibility," in *Proc. IEEE Int. Conf. Veh. Electron. Safety (ICVES)*, 2017, pp. 178–184.

[6] D. Wang, W. Fu, J. Zhou, and Q. Song, "Occlusion-aware motion planning for autonomous driving," *IEEE Access*, vol. 11, pp. 42809–42823, 2023.

[7] B. Gilhuly, A. Sadeghi, P. Yedmellat, K. Rezaee, and S. L. Smith, "Looking for trouble: Informative planning for safe trajectories with occlusions," in *Proc. Int. Conf. Robot. Autom. (ICRA)*, 2022, pp. 8985–8991.

[8] C. Katrakazas, M. Quddus, and W.-H. Chen, "A new integrated collision risk assessment methodology for autonomous vehicles," *Accid. Anal. Prevent.*, vol. 127, pp. 61–79, Jun. 2019. [Online]. Available: https://www.sciencedirect.com/science/article/pii/S0001457518306614

[9] Ö. Ş. Taş and C. Stiller, "Limited visibility and uncertainty aware motion planning for automated driving," in *Proc. IEEE Intell. Veh. Symp. (IV)*, 2018, pp. 1171–1178.

[10] M.-Y. Yu, R. Vasudevan, and M. Johnson-Roberson, "Occlusion-aware risk assessment for autonomous driving in urban environments," *IEEE Robot. Autom. Lett.*, vol. 4, no. 2, pp. 2235–2241, Apr. 2019.

[11] L. Wang, C. F. Lopez, and C. Stiller, "Generating efficient behaviour with predictive visibility risk for scenarios with occlusions," in *Proc. IEEE 23rd Int. Conf. Intell. Transp. Syst. (ITSC)*, 2020, pp. 1–7.

[12] C. Zhang, S. Ma, M. Wang, G. Hinz, and A. Knoll, "Efficient POMDP behavior planning for autonomous driving in dense urban environments using multi-step occupancy grid maps," in *Proc. IEEE 25th Int. Conf. Intell. Transp. Safety (ITSC)*, 2022, pp. 2722–2729.

[13] C. Zhang, F. Steinhauser, G. Hinz, and A. Knoll, "Traffic mirror-aware POMDP behavior planning for autonomous urban driving," in *Proc. IEEE Intell. Veh. Symp. (IV)*, 2022, pp. 323–330.

[14] C. Zhang, F. Steinhauser, G. Hinz, and A. Knoll, "Improved occlusion scenario coverage with a POMDP-based behavior planner for autonomous urban driving," in *Proc. IEEE Int. Intell. Transp. Syst. Conf. (ITSC)*, 2021, pp. 593–600.

[15] C. Hubmann, N. Quetschlich, J. Schulz, J. Bernhard, D. Althoff, and C. Stiller, "A POMDP maneuver planner for occlusions in urban scenarios," in *Proc. IEEE Intell. Veh. Symp. (IV)*, 2019, pp. 2172–2179.

[16] K. H. Wray et al., "POMDPs for safe visibility reasoning in autonomous vehicles," in *Proc. IEEE Int. Conf. Intell. Saf. Robot. (ISR)*, 2021, pp. 191–195.

[17] Y. Wang, Y. Guo, and J. Wang, "A hierarchical planning framework of the intersection with blind zone and uncertainty," in *Proc. IEEE Int. Intell. Transp. Syst. Conf. (ITSC)*, 2021, pp. 687–692.

[18] M. Bouton, A. Nakhaei, K. Fujimura, and M. J. Kochenderfer, "Scalable decision making with sensor occlusions for autonomous driving," in *Proc. IEEE Int. Conf. Robot. Autom. (ICRA)*, 2018, pp. 2076–2081.

[19] D. Wang, W. Fu, Q. Song, and J. Zhou, "Potential risk assessment for safe driving of autonomous vehicles under occluded vision," *Sci. Rep.*, vol. 12, no. 1, p. 4981, 2022.

[20] M. Althoff and S. Magdici, "Set-based prediction of traffic participants on arbitrary road networks," *IEEE Trans. Intell. Veh.*, vol. 1, no. 2, pp. 187–202, Jun. 2016.

[21] M. Koschi and M. Althoff, "Set-based prediction of traffic participants considering occlusions and traffic rules," *IEEE Trans. Intell. Veh.*, vol. 6, no. 2, pp. 249–265, Jun. 2021.

[22] P. F. Orzechowski, A. Meyer, and M. Lauer, "Tackling occlusions limited sensor range with set-based safety verification," in *Proc. 21st Int. Conf. Intell. Transp. Syst. (ITSC)*, 2018, pp. 1729–1736.
[23] H. Park, J. Choi, H. Chin, S.-H. Lee, and D. Baek, "Occlusion-aware risk assessment and driving strategy for autonomous vehicles using simplified reachability quantification," 2023, *arXiv:2306.07004*.
[24] M. Naumann, H. Konigshof, M. Lauer, and C. Stiller, "Safe but not overcautious motion planning under occlusions and limited sensor range," in *Proc. IEEE Intell. Veh. Symp. (IV)*, 2019, pp. 140–145.
[25] Y. Nager, A. Censi, and E. Frazzoli, "What lies in the shadows? Safe and computation-aware motion planning for autonomous vehicles using intent-aware dynamic shadow regions," in *Proc. Int. Conf. Robot. Autom. (ICRA)*, 2019, pp. 5800–5806.
[26] S. Lee, W. Lim, M. Sunwoo, and K. Jo, "Limited visibility aware motion planning for autonomous valet parking using reachable set estimation," *Sensors*, vol. 21, no. 4, p. 1520, Feb. 2021. [Online]. Available: https://doi.org/10.3390/s21041520
[27] Z. Zhang and J. F. Fisac, "Safe occlusion-aware autonomous driving via game-theoretic active perception," in *Proc. Robotics*, 2021, pp. 1–13.
[28] P. Narksri, H. Darweesh, E. Takeuchi, Y. Ninomiya, and K. Takeda, "Occlusion-aware motion planning with visibility maximization via active lateral position adjustment," *IEEE Access*, vol. 10, pp. 57759–57782, 2022.
[29] C. Packer et al., "Is anyone there? Learning a planner contingent on perceptual uncertainty," in *Conf. Robot Learn.*, 2023, pp. 1607–1617. [Online]. Available: https://api.semanticscholar.org/CorpusID:257432830
[30] S. Hoermann, F. Kunz, D. Nuss, S. Renter, and K. Dietmayer, "Entering crossroads with blind corners. A safe strategy for autonomous vehicles," in *Proc. IEEE Intell. Veh. Symp. (IV)*, 2017, pp. 727–732.
[31] J. Müller, J. Strohbeck, M. Herrmann, and M. Buchholz, "Motion planning for connected automated vehicles at occluded intersections with infrastructure sensors," *IEEE Trans. Intell. Transp. Syst.*, vol. 23, no. 10, pp. 17479–17490, Oct. 2022.
[32] V. Narri, A. Alanwar, J. Mårtensson, C. Norén, L. Dal Col, and K. H. Johansson, "Set-membership estimation in shared situational awareness for automated vehicles in occluded scenarios," in *Proc. IEEE Intell. Veh. Symp. (IV)*, 2021, pp. 385–392.
[33] Y. Jeong, J. Yoo, Y. Yoon, and K. Yi, "Collision preventive velocity planning based on static environment representation for autonomous driving in occluded region," in *Proc. IEEE Intell. Veh. Symp. (IV)*, 2020, pp. 425–430.
[34] B. Li, "Occlusion-aware on-road autonomous driving: A trajectory planning method considering occlusions of Lidars," *Optik*, vol. 243, Oct. 2021, Art. no. 167347. [Online]. Available: https://www.sciencedirect.com/science/article/pii/S0030402621009906
[35] B. Li, T. Acarman, Y. Zhang, and Q. Kong, "Occlusion-aware on-road autonomous driving: A path planning method in combination with honking decision making," in *Proc. 33rd Chin. Control Decis. Conf. (CCDC)*, 2021, pp. 7403–7408.
[36] M. Werling, J. Ziegler, S. Kammel, and S. Thrun, "Optimal trajectory generation for dynamic street scenarios in a Frenét frame," in *Proc. IEEE Int. Conf. Robot. Autom.*, 2010, pp. 987–993.
[37] M. Werling, S. Kammel, J. Ziegler, and L. Gröll, "Optimal trajectories for time-critical street scenarios using discretized terminal manifolds," *Int. J. Robot. Res.*, vol. 31, no. 3, pp. 346–359, 2012. [Online]. Available: https://doi.org/10.1177/0278364911423042
[38] M. Geisslinger, P. Karle, J. Betz, and M. Lienkamp, "Watch-and-learn-net: Self-supervised online learning for probabilistic vehicle trajectory prediction," in *Proc. IEEE Int. Conf. Syst., Man, Cybern. (SMC)*, 2021, pp. 869–875.
[39] M. Kaufmann, "The morgan Kaufmann series in interactive 3D technology," in *Real-Time Collision Detection*, C. Ericson, Ed. San Francisco, CA, USA: Morgan Kaufmann, 2005. [Online]. Available: https://www.sciencedirect.com/science/article/pii/B9781558607323500218
[40] M. Geisslinger, F. Poszler, and M. Lienkamp, "An ethical trajectory planning algorithm for autonomous vehicles," *Nat. Mach. Intell.*, vol. 5, pp. 137–144, Feb. 2023.
[41] (Nat. Highway Traffic Safety Admin., Washington, DC, USA). *Crash Report Sampling System*. (2023). [Online]. Available: https://www.nhtsa.gov/crash-data-systems/crash-report-sampling-system
[42] "Definition of harm: Cambridge university press." Cambridge Dictionary. 2023. [Online]. Available: https://dictionary.cambridge.org/dictionary/english/harm
[43] (Bundesministerium für Digitales und Verkehr, Berlin, Germany). *Ethik-Kommission: Automatisiertes und Vernetztes Fahren*. (Jun. 2017). [Online]. Available: https://www.bundesregierung.de/breg-de/service/publikationen/bericht-der-ethik-kommission-729110
[44] E. Petrucelli, J. D. States, and L. N. Hames, "The abbreviated injury scale: Evolution, usage and future adaptability," *Accid. Anal. Prevent.*, vol. 13, no. 1, pp. 29–35, 1981. [Online]. Available: https://www.sciencedirect.com/science/article/pii/0001457581900403
[45] T. A. Gennarelli and E. Wodzin, "AIS 2005: A contemporary injury scale," *Injury*, vol. 37, no. 12, pp. 1083–1091, Dec. 2006.
[46] D. G. Kleinbaum and M. Klein, *Logistic Regression* (Statistics for Biology and Health), 3rd ed. New York, NY, USA: Springer, 2010. [Online]. Available: https://link.springer.com/book/10.1007/978-1-4419-1742-3
[47] M. Geisslinger, F. Poszler, J. Betz, C. Lütge, and M. Lienkamp, "Autonomous driving ethics: From trolley problem to ethics of risk," *Philos. Technol.*, vol. 34, pp. 1033–1055, Apr. 2021.
[48] R. Trauth, P. Karle, T. Betz, and J. Betz, "An end-to-end optimization framework for autonomous driving software," in *Proc. 3rd Int. Conf. Comput., Control Robot. (ICCCR)*, 2023, pp. 137–144.
[49] R. Trauth, M. Kaufeld, M. Geisslinger, and J. Betz, "Learning and adapting behavior of autonomous vehicles through inverse reinforcement learning," in *Proc. IEEE Intell. Veh. Symp. (IV)*, 2023, pp. 1–8.
[50] (Bundesministerium für Digitales und Verkehr, Berlin, Germany). *Verkehr in Zahlen 2022/2023*. (2022). [Online]. Available: https://bmdv.bund.de/SharedDocs/DE/Publikationen/G/verkehr-in-zahlen-2022-2023-pdf.html
[51] H. Schüller, M. Niestegge, M. Roßmerkel, J. Schade, L. Rößger, and K. Rehberg, *Systematische Untersuchung sicherheitsrelevanten Fußgängerverhaltens, Bericht zum Forschungsprojekt 82.0689*, Fachverlag NW in der Carl Ed. Schünemann KG, Bergisch Gladbach, Germany, 2020.
[52] (Nat. Highway Traffic Safety Admin., Washington, DC, USA). *Fatality Analysis Reporting System*. (2023). [Online]. Available: https://www.nhtsa.gov/crash-data-systems/fatality-analysis-reporting-system
[53] (Insur. Inst. Highway Safety, Virginia, USA). *Fatality facts 2021, Pedestrians*. (2021). [Online]. Available: https://www.iihs.org/topics/fatality-statistics/detail/pedestrians
[54] M. Althoff, M. Koschi, and S. Manzinger, "CommonRoad: Composable benchmarks for motion planning on roads," in *Proc. IEEE Intell. Veh. Symp. (IV)*, 2017, pp. 719–726.
[55] R. Firoozi, A. Mir, G. S. Camps, and M. Schwager, "Occlusion-aware MPC for guaranteed safe robot navigation with unseen dynamic obstacles," 2022, *arXiv:2211.09156*.
[56] P. Trautman and A. Krause, "Unfreezing the robot: Navigation in dense, interacting crowds," in *Proc. IEEE/RSJ Int. Conf. Intell. Robots Syst.*, 2010, pp. 797–803.
[57] M. Geisslinger, R. Trauth, G. Kaljavesi, and M. Lienkamp, "Maximum acceptable risk as criterion for decision-making in autonomous vehicle trajectory planning," *IEEE Open J. Intell. Transp. Syst.*, vol. 4, pp. 570–579, 2023.

RAINER TRAUTH received the B.Sc. degree in engineering science and the M.Sc. degree in mechanical engineering from the Technical University of Munich in 2017 and 2020, respectively, where he is currently pursuing the Ph.D. degree in mechanical engineering with the Institute of Automotive Technology. His research interests include motion planning, situational awareness, and behavior planning approaches focusing on real-world applications in autonomous driving.

KORBINIAN MOLLER received the B.Sc. degree in mechanical engineering from the Technical University of Munich (TUM) in 2021, and the M.Sc. degree in mechanical engineering from the TUM School of Engineering and Design in 2023. He is currently pursuing the Ph.D. degree with the Autonomous Vehicle Systems Lab, TUM. His research interests include vehicle dynamics simulation, optimization of electric drivetrains, and motion planning in autonomous driving.

JOHANNES BETZ (Member, IEEE) received the B.Eng. degree from the University of Applied Science Coburg in 2011, the M.Sc. degree from the University of Bayreuth in 2012, and the Ph.D. degree and the M.A. degree in philosophy from Technical University of Munich (TUM) in 2019 and 2021, respectively. He is an Assistant Professor with the Department of Mobility Systems Engineering, TUM, where he is leading the Autonomous Vehicle Systems Lab. He is one of the Founder of the TUM Autonomous Motorsport Team. His research focuses on developing adaptive dynamic path planning and control algorithms, decision-making algorithms that work under high uncertainty in multiagent environments, and validating the algorithms on real-world robotic systems.